A PETROV-GALERKIN METHOD WITH A NATURAL DISCONTINUITY CAPTURING OPERATOR: APPLICATION TO CONVECTION-DIFFUSION PROBLEMS

Paulo A. B. de Sampaio – sampaio@cnen.gov.br
Instituto de Engenharia Nuclear – CNEN
Cx. P. 68550 - 21945-970 - Rio de Janeiro, RJ, Brazil
Álvaro L.G.A. Coutinho – alvaro@coc.ufrj.br
Center for Parallel Computing and Dept. of Civil Engineering, COPPE/UFRJ
Cx. P. 68506 – 21945-970 - Rio de Janeiro, RJ, Brazil

Abstract. *The concept of effective transport velocity is introduced to derive a discontinuity capturing operator for convection-diffusion problems. The effective transport velocity, which depends both on the flow velocity and on the local solution gradient, is used to modify the classical representation of the convective term. As a result, the discontinuity capturing operator arises naturally in the derivation of a Petrov-Galerkin method obtained via a least-squares approach. The weighting functions thus obtained introduce stabilising terms acting both on the streamline and the gradient directions. The numerical examples presented demonstrate the effectiveness of the proposed method. These include the classical problem of the advection of a steep profile skew to the mesh and the computation of the temperature field in a free convection problem.*

Keywords: *Stabilised Formulations, Petrov-Galerkin Methods, Convection-Diffusion.*

1. INTRODUCTION

The Galerkin method is ill suited for the analysis of convection dominated problems. The so-called *best approximation property,* which the Galerkin formulation exhibits for self-adjoint operators, is lost whenever convection terms are present. In practice, the application of the Galerkin formulation to convective problems results in spatial oscillations (wiggles) that may pollute the solution on the whole analysis domain.

A major advance was obtained with the development of the *Streamline Upwind Petrov-Galerkin (SUPG)* method (Brooks & Hughes, 1982), also known as *Anisotropic Balancing Dissipation* (Kelly *et al.*, 1980). In such method upwinding is introduced along streamlines and a stabilising diffusive term, acting only on the streamline direction, is generated. Hence the name *Anisotropic Balancing Dissipation*. Most importantly, this effect is achieved within the framework of consistent Petrov-Galerkin formulations. Other successful finite element approaches to the solution of convection dominated problems, such as the Taylor-Galerkin (Donea, 1984), Characteristic-Galerkin (Lohner *et al.*, 1984) and least-squares based methods

(Carey & Jiang, 1988), (De Sampaio,1991), can be also shown to be consistent Petrov-Galerkin formulations.

The SUPG method presents good stability and accuracy if the exact solution is regular. For non-regular solutions, though, localised wiggles may appear in regions containing sharp layers, unresolvable on the finite element mesh. Hughes *et al.*(1986) addressed this problem adding an extra perturbation to the SUPG weighting function. The effect of this extra weighting is to create a *Discontinuity Capturing Operator*, which introduces diffusion along the direction of the solution gradient. Improved results were obtained near sharp layers, at the expense of introducing a non-linear mechanism to the computation of the Petrov-Galerkin weighting functions. Galeão and Do Carmo (1988) pursued this line of research further, attempting to define the most appropriate upwind direction. The Streamline and the Discontinuity Capturing Operators were later generalised to multi-dimensional advective-diffusive systems in the works of Hughes & Mallet (1986).

In this paper the scope is restricted to the transient multi-dimensional convection-diffusion equation. In section 2, we review the derivation of a Petrov-Galerkin method based on a least-squares approximation of the time-discretised convection-diffusion problem (De Sampaio, 1991). This allows relating the time-step used in the time discretisation with the so-called intrinsic time-scales and upwind parameters. In section 3, we introduce the concept of *effective transport velocity* to obtain a natural derivation of the discontinuity-capturing operator. The *effective transport velocity* depends on the flow velocity and on the solution gradient. The resulting discontinuity-capturing operator does not create the undesirable doubling effect of the original SUPG+discontinuity capturing formulation, thus avoiding *ad hoc* corrections. Numerical examples are presented in section 4. The first example is the classical problem of the advection of a steep profile using a velocity field skew to the mesh. Next, we show the method working within our Navier-Stokes finite element program (De Sampaio & Coutinho, 1999), in the computation of the temperature field in a free convection problem. The effectiveness of the present approach in controlling wiggles is demonstrated.

Finally, concluding remarks are presented in section 5.

2. A LEAST-SQUARES BASED PETROV-GALERKIN METHOD

Let us consider the conservation of energy for an incompressible flow. The problem is defined on the open bounded domain Ω, with boundary Γ, contained in the *nsd*-dimensional Euclidean space. The energy equation is written using the summation convention for *b=1,...,nsd* , in Cartesian co-ordinates, as

$$\rho c\left[\frac{\partial T}{\partial t}+\frac{\partial}{\partial x_b}\left(u_b T\right)\right]+\frac{\partial q_b}{\partial x_b}-Q=0 \tag{1}$$

In the above equation T is temperature, u_b is the flow velocity and Q is a volumetric heat source. Density and specific heat are denoted by ρ and c, respectively. The heat-flux is defined according to Fourier's law by $q_b=-\kappa\,\partial T/\partial x_b$, where κ is the thermal conductivity. Fluid properties are assumed constant throughout.

As the flow is assumed incompressible, i.e. $\partial u_b/\partial x_b=0$, we can also write the energy balance Eq.(1) as a typical convection-diffusion equation,

$$\rho c\left[\frac{\partial T}{\partial t}+u_b\frac{\partial T}{\partial x_b}\right]+\frac{\partial q_b}{\partial x_b}-Q=0 \tag{2}$$

The problem boundary conditions are prescribed temperature and heat-flux, $\overline{T}$ and $\overline{q}$, respectively. These are specified on non-overlapping parts of the boundary Γ_T and Γ_q, such that $T = \overline{T}$ on Γ_T and $q_b\ n_b = \overline{q}$ on Γ_q. Note that n_b denotes the outward normal to the surface.

2.1 Discretisation

Here we consider a least-squares approach to approximating the energy convection-diffusion equation. The method is similar to that employed by Carey & Jiang (1988) for hyperbolic problems. In the present case, though, we need to introduce the second order spatial derivatives corresponding to diffusive effects.

In order to derive the method, let us define the energy squared residuals as

$$S = \int_\Omega \left(\hat{R}^{n+\theta}\right)^2 \, d\Omega \tag{3}$$

where

$$\hat{R}^{n+\theta} = \rho c \left(\frac{\hat{T}^{n+1} - \hat{T}^n}{\Delta t} + \hat{u}_a^n \frac{\partial \hat{T}^{n+\theta}}{\partial x_a} \right) + \frac{\partial q_a^{n+1/2}}{\partial x_a} - \hat{Q}^{n+1/2} \tag{4}$$

The superscripts in the above equations denote the time-level. Note that θ, varying from zero to one, parameterises time between the time level *n* and the time-level *n+1*, respectively. The time-step is denoted by $\Delta t = t^{n+1} - t^n$. Furthermore, $\hat{T}$, $\hat{u}_a$ and $\hat{Q}$ are interpolated fields corresponding to temperature, velocity and volumetric heat source, respectively. These fields are interpolated using standard C_0 element shape functions denoted by N_i. For the time being we do not specify any particular spatial discretisation for $q_a^{n+1/2}$ and treat the heat flux contribution as a source term.

Minimising S with respect to the free temperature parameters we obtain

$$\int_\Omega \left(N_i + \theta \, \Delta t \;\, u_b^n \frac{\partial N_i}{\partial x_b} \right) \hat{R}^{n+\theta} \; d\Omega \; = \; 0 \qquad \forall \text{ free } T_i^{n+1} \tag{5}$$

Note that Eq.(5) states a Petrov-Galerkin weighted residual formulation. It still has to be modified to include the heat-flux boundary condition. Recalling that $q_b\ n_b = \overline{q}$ on Γ_q, the following result is obtained after using Green's identity to rewrite the Galerkin diffusive contribution to Eq.(5):

$$\begin{aligned} &\int_\Omega \left(N_i + \theta \, \Delta t \, \hat{u}_b{}^n \frac{\partial N_i}{\partial x_b} \right) \left(\rho c \left(\frac{\hat{T}^{n+1} - \hat{T}^n}{\Delta t} \right) + \rho c \, \hat{u}_a{}^n \frac{\partial \hat{T}^{n+\theta}}{\partial x_a} - \hat{Q}^{n+1/2} \right) d\Omega \quad + \\ & - \int_\Omega \frac{\partial N_i}{\partial x_a} \, q_a{}^{n+1/2} \, d\Omega \; + \int_{\Gamma_q} N_i \, \overline{q} \; d\Gamma \; + \int_\Omega \theta \, \Delta t \, \hat{u}_b{}^n \frac{\partial N_i}{\partial x_b} \frac{\partial q_a{}^{n+1/2}}{\partial x_a} \; d\Omega \quad = \quad 0 \end{aligned} \tag{6}$$

At this point we have to introduce the spatial discretisation of the heat flux. Based on Fourier's law, this is expressed in terms of the discretised temperature field as

$$\hat{q}_a^{n+1/2} = -\kappa \frac{\partial \hat{T}^{n+1/2}}{\partial x_a} \tag{7}$$

The shape functions N_i have C_0 continuity. Therefore, in view of the above discretisation of the heat-flux, the last term in Eq.(6) is not well defined on element interfaces. In practice this term is evaluated on the element interiors Ωe, where it has the required regularity. The resulting approximation is given by

$$\begin{aligned} &\int_\Omega \left(N_i + \theta\, \Delta t\, \hat{u}_b{}^n \frac{\partial N_i}{\partial x_b} \right) \left(\rho c \left(\frac{\hat{T}^{n+1} - \hat{T}^n}{\Delta t} \right) + \rho c\, \hat{u}_a{}^n \frac{\partial \hat{T}^{n+\theta}}{\partial x_a} - \hat{Q}^{n+1/2} \right) d\Omega \quad + \\ &\int_\Omega \frac{\partial N_i}{\partial x_a}\, \kappa \frac{\partial \hat{T}}{\partial x_a}^{n+1/2} d\Omega \; - \sum_{\Omega e} \int_{\Omega e} \theta\, \Delta t\, \hat{u}_b{}^n \frac{\partial N_i}{\partial x_b} \frac{\partial}{\partial x_a} \left(\kappa \frac{\partial \hat{T}}{\partial x_a} \right)^{n+1/2} d\Omega \; = -\int_{\Gamma_q} N_i\, \bar{q}\, d\Gamma \end{aligned} \tag{8}$$

It is important to remark that the Petrov-Galerkin formulation above leads to symmetric systems if linear elements are used, i.e., linear triangles in 2D or linear tetrahedra in 3D.

2.2 Optimal time-steps

Note that the weighting function applied to energy balance, Eq.(5), has the *streamline upwind Petrov-Galerkin* structure (Brooks & Hughes, 1982). For $\theta = 1/2$ we have,

$$W_i = N_i + \frac{\Delta t}{2}\, \hat{u}_b{}^n \frac{\partial N_i}{\partial x_b} \tag{9}$$

For linear elements, a proper amount of *streamline upwinding* is introduced choosing the time-step as

$$\Delta t = \alpha \frac{h_e}{\left\| \mathbf{u^n} \right\|} \tag{10}$$

where

$$\alpha = \left[\coth\left(\frac{Pe}{2} \right) - \frac{2}{Pe} \right] \tag{11}$$

In the above equations $\left\| \mathbf{u^n} \right\| = \sqrt{u_a{}^n\, u_a{}^n}$ is the local velocity modulus and h_e is the characteristic element size (the square root of the element area). The element Peclet number is $Pe = \rho c \left\| \mathbf{u^n} \right\| h_e / \kappa$.

Note that α, defined by Eq.(11), is the so-called optimal upwind parameter, whose choice leads to nodally exact solutions for one-dimensional steady-state problems.

The time-step given by Eq.(10), associated to the optimal upwind parameter, is appropriate to follow the time evolution of the convection-diffusion processes resolvable in a mesh with size h_e (De Sampaio, 1991). Indeed, Eq.(10) yields $\Delta t = h_e / \|\mathbf{u}^n\|$ in the pure convection limit ($Pe \to \infty$), whereas for pure diffusion ($Pe = 0$) it yields $\Delta t = \rho c\, h_e^2 / 6k$.

The relationship between the time-step given by Eq.(10), also called the *intrinsic time scale*, and the modelling of the sub-grid (or unresolvable) scales was investigated by Hughes (1995). It is important to remark that the time-step calculated from the optimal upwind parameter α varies from element to element, according to the local velocity and mesh size. Thus, one has to use local time-stepping to get accurate steady-state solutions via pseudo transients. In cases where real transient solutions are sought, special algorithms are required to accommodate the use of these spatially varying time-steps (De Sampaio, 1993).

3. DISCONTINUITY CAPTURING

In this section we shall present a simple and natural way to introducing a discontinuity capturing operator in the method presented in section 2.

Let us consider a velocity field **w** aligned with the temperature gradient direction, as depicted in Fig.1. This velocity field, which we call *the effective transport velocity*, is defined according to the following expression:

$$\mathbf{w} = \left(\frac{\mathbf{u} \cdot \nabla T}{\|\nabla T\|} \right) \frac{\nabla T}{\|\nabla T\|} \tag{12}$$

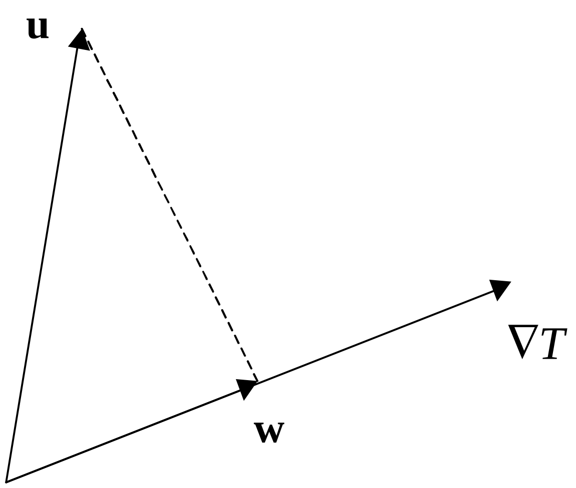

Figure 1 - The effective transport velocity $\mathbf{w}$.

Obviously, **w** is defined only where a temperature gradient exists. In particular, note that the name *effective transport velocity* comes from the fact that $\mathbf{w} \cdot \nabla T = \mathbf{u} \cdot \nabla T$. We can also define a velocity field **v**, combining the flow velocity field **u** and the velocity **w** given by Eq.(12). This velocity field can be written as $\mathbf{v} = \gamma \mathbf{u} + (1-\gamma)\mathbf{w}$, where $0 \le \gamma \le 1$. The parameter γ is chosen to be $\gamma = 1$ wherever $\|\nabla T\| = 0$, ensuring that the field **v** is always well defined. Most importantly, the convective term can be rewritten using the velocity **v** instead of the flow velocity **u**, as $\mathbf{v}\cdot\nabla T=\mathbf{u}\cdot\nabla T$.

In the sequel the derivation of the method presented in section 2 is repeated, this time with $\mathbf{v}\cdot\nabla T$ in place of $\mathbf{u}\cdot\nabla T$. We shall see that the resulting Petrov-Galerkin formulation embedds a discontinuity capturing operator.

3.1 A Petrov-Galerkin/least-squares method embedding discontinuity capturing

Using the velocity field **v**, the residual $\hat{R}^{n+\theta}$ given by Eq.(4) can be recast as

$$\hat{R}^{n+\theta}=\rho c\left(\frac{\hat{T}^{n+1}-\hat{T}^{n}}{\Delta t}+\hat{v}_a^n\frac{\partial\hat{T}^{n+\theta}}{\partial x_a}\right)+\frac{\partial q_a^{n+1/2}}{\partial x_a}-\hat{Q}^{n+1/2} \tag{13}$$

Therefore, using the least-squares procedure presented in section 2.1, we obtain the following Petrov-Galerkin formulation

$$\begin{aligned}&\int_\Omega\left(N_i+\theta\,\Delta t\,\hat{v}_b{}^n\frac{\partial N_i}{\partial x_b}\right)\left(\rho c\left(\frac{\hat{T}^{n+1}-\hat{T}^{n}}{\Delta t}\right)+\rho c\,\hat{v}_a{}^n\frac{\partial\hat{T}^{n+\theta}}{\partial x_a}-\hat{Q}^{n+1/2}\right)d\Omega\quad+\\&\int_\Omega\frac{\partial N_i}{\partial x_a}\,\kappa\frac{\partial\hat{T}}{\partial x_a}^{n+1/2}d\Omega-\sum_{\Omega e}\int_{\Omega e}\theta\,\Delta t\,\hat{v}_b{}^n\frac{\partial N_i}{\partial x_b}\frac{\partial}{\partial x_a}\left(\kappa\frac{\partial\hat{T}}{\partial x_a}\right)^{n+1/2}d\Omega=-\int_{\Gamma_q}N_i\,\bar{q}\,d\Gamma\end{aligned} \tag{14}$$

Like Eq.(8), note that Eq.(14) is symmetric for linear triangles in 2D and for linear tetrahedra in 3D. Most importantly, rather than introducing dissipation in the streamline direction only, i.e., the direction of the flow velocity **u**, the Petrov-Galerkin formulation above introduces dissipation in the direction of the velocity field **v**.

It is a simple matter to show that Eq.(14) embeds both the streamline upwinding and the discontinuity capturing operators. These operators arise from the interaction between the non-Galerkin part of the weighting function and the convective term, as indicated below

$$\begin{aligned}&\int_\Omega\theta\,\Delta t\,\hat{v}_b{}^n\frac{\partial N_i}{\partial x_b}\left(\rho c\,\hat{v}_a{}^n\frac{\partial\hat{T}^{n+\theta}}{\partial x_a}\right)d\Omega=\\&\theta\,\Delta t\,\rho c\left[\gamma^2\int_\Omega\left(\hat{u}_b{}^n\frac{\partial N_i}{\partial x_b}\right)\left(\hat{u}_a{}^n\frac{\partial\hat{T}^{n+\theta}}{\partial x_a}\right)d\Omega+(1-\gamma)^2\int_\Omega\left(\hat{w}_b{}^n\frac{\partial N_i}{\partial x_b}\right)\left(\hat{w}_a{}^n\frac{\partial\hat{T}^{n+\theta}}{\partial x_a}\right)d\Omega\right]+\\&\theta\,\Delta t\,\rho c\;\gamma(1-\gamma)\left[\int_\Omega\left(\hat{w}_b{}^n\frac{\partial N_i}{\partial x_b}\right)\left(\hat{u}_a{}^n\frac{\partial\hat{T}^{n+\theta}}{\partial x_a}\right)d\Omega+\int_\Omega\left(\hat{u}_b{}^n\frac{\partial N_i}{\partial x_b}\right)\left(\hat{w}_a{}^n\frac{\partial\hat{T}^{n+\theta}}{\partial x_a}\right)d\Omega\right]\end{aligned} \tag{15}$$

The first integral on the right hand side of Eq.(15) is the streamline diffusion operator, whilst the second integral is the discontinuity capturing operator. Note that the discontinuity capturing operator has the same structure of the one introduced by Hughes, Mallet & Mizukami (1986). However, in (Hughes et al., 1986) the streamline and the discontinuity capturing operators are always superimposed. This means that an undesirable *doubling effect*, causing excessive diffusion if **u** and ∇T are aligned, requires some special *ad hoc* correction.

This is unnecessary for the method presented herein: the summation of the two operators add to the correct amount of directional diffusion in case the alignment of **u** and ∇T does occur.

The criterion to select the time-step is the same described in section 2.2, but now using **v** rather than **u** in Eq.(10)-(11). The Peclet number used to compute α is also redefined in terms of **v**, i.e., $Pe = \rho c \left\| \mathbf{v}^{\mathbf{n}} \right\| h_e / \kappa$.

We must also choose the γ parameter. One can devise a scheme where $\gamma = 1$ in regular regions (only streamline upwinding) but switching to $\gamma = 0.5$ in regions containing sharp layers, in order to activate both operators in such regions. Other alternatives are possible: in the examples shown in section 4 we have chosen $\gamma = 0.5$, changing to $\gamma = 1$ only if the temperature gradient vanishes locally.

4. NUMERICAL EXAMPLES

The following numerical examples demonstrate the effectiveness of the proposed method in controlling wiggles.

The first example is the classical problem of the advection of a steep profile by a velocity field skew to the mesh. This is a two-dimensional steady state high convection problem with a uniform velocity field. The analysis domain is a square with side *L*, as indicated in Fig.2. The global Peclet number is $P = \rho c \left\| \mathbf{u} \right\| L / \kappa = 10^8$.

The temperature boundary condition on the left face is

$$T(-0.5L, y) = \begin{cases} 0 & \text{for} \quad -0.50L \le y < -0.30L \\ 20y + 6 & \text{for} \quad -0.30L \le y < -0.25L \\ 1 & \text{for} \quad -0.25L \le y < 0.45L \\ -20y + 10 & \text{for} \quad 0.45L \le y \le 0.50L \end{cases} \tag{16}$$

Homogeneous temperature boundary conditions (*T=0*) are imposed on the other faces.

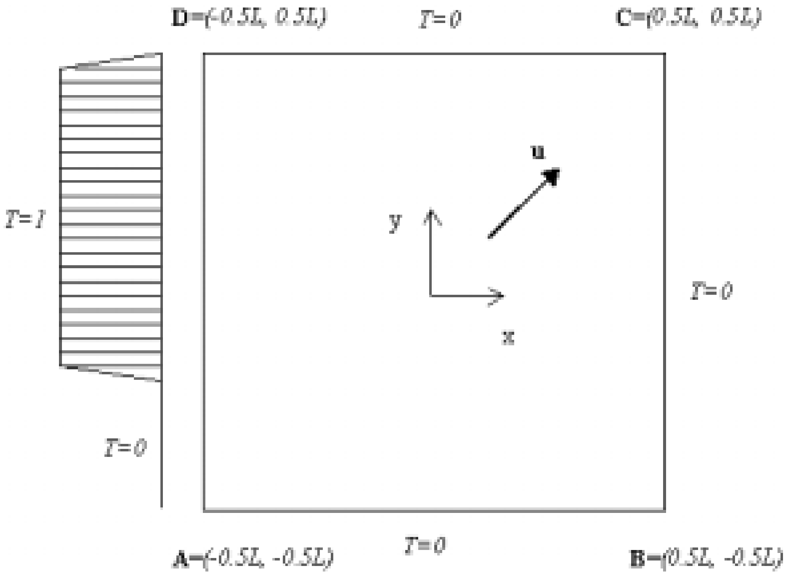

Figure 2 - Advection of a steep temperature profile: domain and boundary conditions.

Considering the global Peclet number of 10^8 and the given boundary conditions, the exact solution will have the following properties: a) virtually no smearing of the profile imposed on the left face, as this profile is advected to the interior of the domain. b) there will be a sharp boundary layer at the top face, where the internal solution must drop to zero in order to satisfy the boundary condition imposed there.

For this steady-state example we have used $\theta = 1$. Computations were made with $\mathbf{u}$ aligned to directions (1,1) and (2,1). For each of these directions we present results obtained with $\gamma = 1$, i.e., without discontinuity capturing, and with $\gamma = 0.5$, where both the streamline upwinding and discontinuity capturing operators are active.

The numerical results can be seen in Figures 3 and 4. These are presented in the form of temperature elevations viewed from the downstream corner **C** shown in Fig.2. Note that wiggles are responsible for unrealistic temperature values, lower than zero or higher than one, in the analyses performed. The proposed method, with $\gamma = 0.5$, yields sharp solutions with much better control of wiggles than the results obtained with $\gamma = 1$.

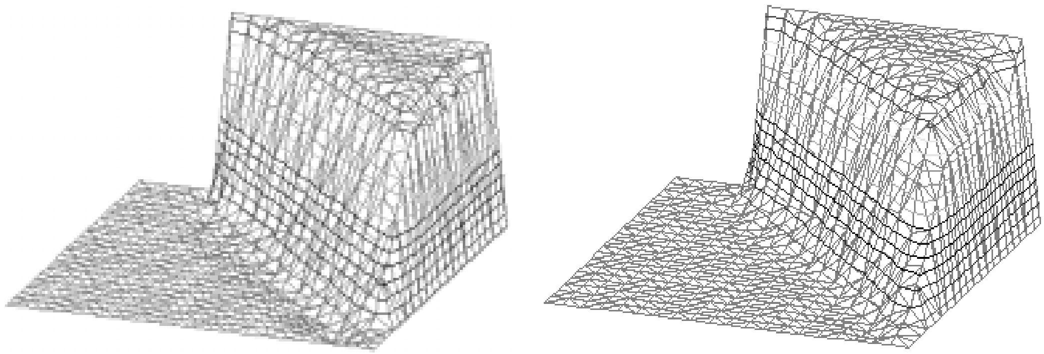

(a) *Min.* -0.061478 *Max.* 1.037047

(b) *Min.* -0.024390 *Max.* 1.011613

Figure 3 - Advection of a steep temperature profile: velocity aligned to direction (1,1). (a) temperature obtained with $\gamma = 1$. (b) temperature obtained with $\gamma = 0.5$.

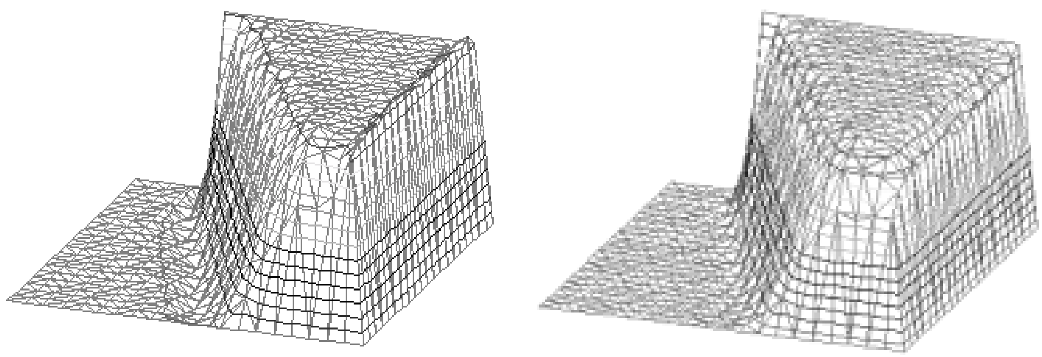

(a) *Min.* -0.085208 *Max.* 1.143970

(b) *Min.* -0.027058 *Max.* 1.008273

Figure 4 - Advection of a steep temperature profile: velocity aligned to direction (2,1). (a) temperature obtained with $\gamma = 1$. (b) temperature obtained with $\gamma = 0.5$.

In the next example we simulate the external free convection flow that develops around a hot horizontal pipe with external diameter *D*. The temperature of the pipe surface exceeds that of the surrounding fluid by ΔT. We have used the method presented in section 3, working within our incompressible Navier-Stokes solver (De Sampaio & Coutinho, 1999), to approximate the convection-diffusion of energy. It is important to note that temperature wiggles create spurious sources and sinks of momentum that affect the computation of the flow field in free convection problems. Thus, there is a special need for controlling wiggles in free convection analyses.

The problem is parameterised by the non-dimensional groups of Grashof and Prandtl, given by $Gr = \rho^2 \|\mathbf{g}\| \beta \, \Delta T \, D^3 / \mu^2$ and $Pr = c\mu/\kappa$, respectively. Note that $\mathbf{g}$ is the gravity acceleration and β is the volumetric thermal expansion coefficient. The fluid properties of viscosity, specific heat at constant pressure and thermal conductivity are denoted by μ, c and κ, respectively.

For this transient problem the fluid is considered initially at rest. The initial non-dimensionalised fluid temperature is $T^* = 0$. The non-dimensionalised temperature at the pipe surface is maintained at $T^* = 1$ as a fixed boundary condition. Computations have been performed with $Gr = 10^8$ and Pr=0.72. We have chosen $\theta = 0.5$ for better transient accuracy. Analyses have been made using both $\gamma = 1$ and $\gamma = 0.5$.

Figure 5 presents temperature iso-lines close to the cylinder surface at time $t = 30 \, D^{1/2} / \left(\beta \, \Delta T \|\mathbf{g}\|\right)^{1/2}$. Note the presence of spurious iso-lines and unrealistic temperatures (higher than one or lower than zero) for the run without discontinuity capturing, i.e., $\gamma = 1$. Note that the results obtained using $\gamma = 0.5$, corresponding to streamline upwinding plus discontinuity capturing, are much better.

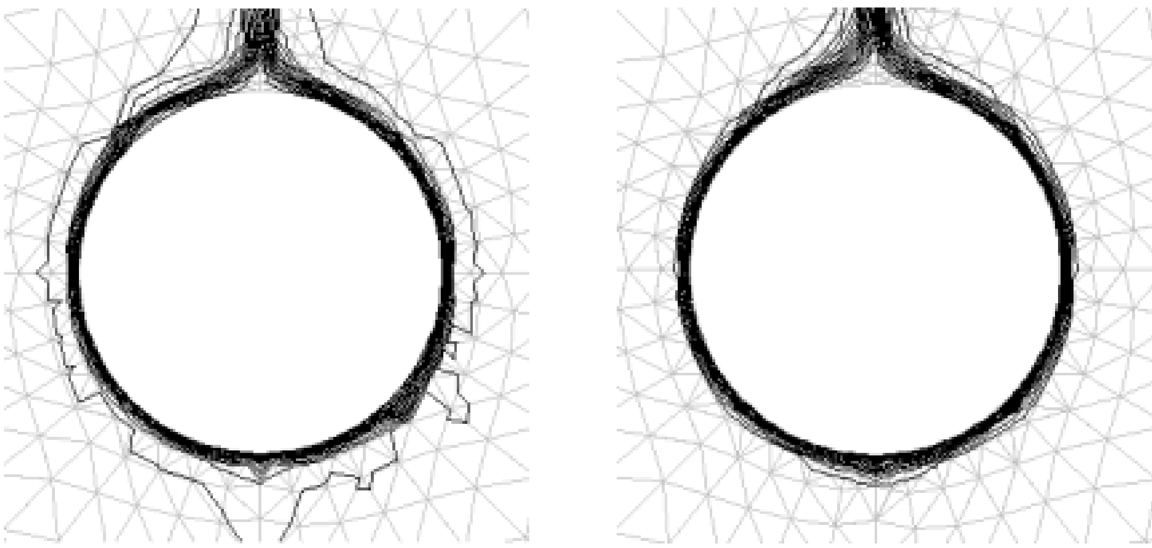

(a) *Min.* -0.067249 *Max.* 1.058100

(b) *Min.* -0.009269 *Max.* 1.009018

Figure 5. Free convection around a hot pipe ($Gr = 10^8$; $Pr = 0.72$): (a) temperature isolines obtained with $\gamma = 1$. (b) temperature isolines obtained with $\gamma = 0.5$.

5. CONCLUDING REMARKS

A natural derivation of a discontinuity capturing for convection-diffusion problems has been presented. This derivation is based on the concept of *effective transport velocity,* which depends both on the flow velocity and on the solution gradient, and on the use of a Petrov-Galerkin/least-squares formulation. The numerical examples shown clearly demonstrate the effectiveness of the method in controlling undesirable wiggles.

REFERENCES

Brooks, A. & Hughes, T.J.R., 1982, Streamline upwind Petrov-Galerkin formulations for convection dominated flows with particular emphasis on the incompressible Navier-Stokes equations, Comput. Methods Appl. Mech. Eng., vol. 32, pp.199-259.

Carey, G.F. & Jiang, B.N., 1988, Least-squares finite elements for first order hyperbolic systems, Int. J. Numer. Methods Eng., vol. 26, pp. 81-93.

De Sampaio, P.A.B., 1991, A Petrov-Galerkin formulation for the incompressible Navier-Stokes equations using equal order interpolation for velocity and pressure, Int. J. Numer. Methods Eng., vol. 31, pp. 1135-1149.

De Sampaio, P.A.B., 1993, Transient solutions of the incompressible Navier-Stokes equations in primitive variables employing optimal local time stepping, Proceedings of the 8th International Conference on Numerical Methods for Laminar and Turbulent Flow, July 18-23, Swansea, pp. 1493-1504.

De Sampaio, P.A.B. & Coutinho, A.L.G.A., 1999, Simulation of free and forced convection incompressible flows using an adaptive parallel/vector finite element procedure, Int. J. Numer. Methods Fluids, vol. 29, pp. 289-309.

Donea, J., 1984, A Taylor-Galerkin method for convective transport problems, Int. J. Numer. Methods Eng., vol. 20, pp. 101-119.

Galeão, A.C. & Do Carmo, E.G.D., 1988, A consistent approximate upwind Petrov-Galerkin Method for convection dominated problems, Comput. Methods Appl. Mech. Eng., vol. 68, pp.83-95.

Hughes, T.J.R., Mallet, M. & Mizukami, A., 1986, A new finite element formulation for computational fluid dynamics: II. Beyond SUPG, Comput. Methods Appl. Mech. Eng., vol. 54, pp. 341-355.

Hughes, T.J.R. & Mallet, M., 1986, A new finite element formulation for computational fluid dynamics: III. The generalized streamline operator for multidimensional advective-diffusive systems, Comput. Methods Appl. Mech. Eng., vol. 58, pp. 305-328.

Hughes, T.J.R. & Mallet, M., 1986, A new finite element formulation for computational fluid dynamics: IV. A discontinuity-capturing operator for multidimensional advective -diffusive systems, Comput. Methods Appl. Mech. Eng., vol. 58, pp. 329-336.

Hughes, T.J.R., 1994, Multiscale phenomena: Green's functions, subgrid scale models, bubbles, and the origins of stabilized methods, Proceedings of the 9th International Conference on Finite Elements in Fluids, Venezia, pp. 99-114.

Kelly, D.W., Nakazawa, S. & Zienkiewicz, O.C., 1980, A note on anisotropic balancing dissipation in the finite element method approximation to convective diffusion problems, Int. J. Numer. Methods Eng., vol. 15, pp. 1705-1711.

Lohner, R., Morgan, K. & Zienkiewicz O.C., 1984, The solution of non-linear hyperbolic equation systems by the finite element method, Int. J. Numer. Methods Fluids, vol. 4, pp. 1043-1063.